Non-destructive monitoring of dye depth profile in mesoporous TiO_2 electrodes of solar cells with micro-SORS

Alessandra Botteon[1,2], Wang-Hyo Kim[3,4], Chiara Colombo[1], Marco Realini[1], Chiara Castiglioni[2], Pavel Matousek[5], Byung-Man Kim[3,4*], Tae-Hyuk Kwon[3,4*], Claudia Conti[1*]

[1]*Institute of Heritage Science (ISPC), National Research Council (CNR), Via Cozzi 53, 20125, Milano, Italy.*

[2] *Department of Chemistry, Materials and Chemical Engineering "G. Natta", Politecnico di Milano, piazza Leonardo da Vinci 32, 20133 Milano, Italy.*

[3]*Department of Chemistry, Ulsan National Institute of Science and Technology (UNIST), Ulsan 44919, Republic of Korea.*

[4]*Center for Wave Energy Materials, UNIST, Ulsan 44919, Republic of Korea.*

[5] *Central Laser Facility, Research Complex at Harwell, STFC Rutherford Appleton Laboratory, UK Research and Innovation (UKRI), Harwell Oxford, OX11 0QX, United Kingdom.*

*Corresponding authors: Byung-Man Kim, kbm30003000@gmail.com; Tae-Hyuk Kwon, kwon90@unist.ac.kr, www.kwon90@com; Claudia Conti, claudia.conti@cnr.it;

ABSTRACT

The dye distribution within a photo-electrode is a key parameter determining the performances of dye-sensitized photon-to-electron conversion devices, such as dye-sensitized solar cell (DSSC). Traditional, depth profiling investigation by destructive means including cross-sectional sampling is unsuitable for large quality control applications in manufacturing processes. Therefore, the non-destructive monitoring of the dye depth profile is required, which is the first step toward a non-destructive evaluation of the internal degradation of device in the field. Here we present a conceptual demonstration of ability to monitor the dye depth profile within the light active layer of DSSC by non-destructive means with high chemical specificity using a recently developed non-destructive/non-invasive Raman method, micro-Spatially Offset Raman Spectroscopy (micro-SORS). Micro-SORS is able to probe through turbid materials providing the molecular identification of compounds located under the surface, without the need of resorting to a cross-sectional analysis. The study was performed on the photo-electrode of DSSCs. This represents the first demonstration of the micro-SORS

concept in the solar cell area as well as, more generally, the application of micro-SORS to the thinnest layer to date. A sample set has been prepared with varying concentration of the dye and the thickness of the matrix consisting of a titanium dioxide layer. The results showed that micro-SORS can unequivocally discriminate between the even and uneven dye depth profiles. Moreover, micro-SORS outcomes have been compared with the results obtained with destructive Time-of-Flight Secondary Ion Mass Spectrometry (TOF-SIMS) measurements. The results of the two techniques are in good agreement, confirming the reliability of micro-SORS analysis. Therefore, this study is expected to open prospects for characterising also depth of the change and its magnitude in the future and paving way for establishing wider and more effective monitoring capability in this important field.

ABSTRACT GRAPHICS

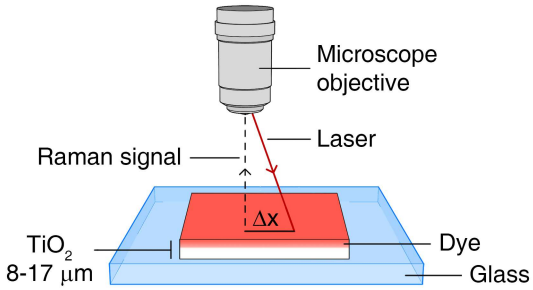

INTRODUCTION

Dye-sensitized photon-to-electron conversion systems including dye-sensitized solar cells (DSSCs), dye-sensitized photo-rechargeable batteries and dye-sensitized photo-electrochemical cells have been investigated as one of the most promising photo-electronic devices using outdoor light, and especially dim indoor light. [1-9] The dye distribution inside the semi-conducting layer is significantly influential for the device performance. For that reason, the state of dye distribution inside titanium dioxide (TiO_2) film has been studied by several methods, but prevalently based on destructive approaches [10-16], that are not suitable for monitoring the internal state of the devices under *in-operando* conditions. Therefore, it is essential to develop non-destructive protocols for extensive applications, such as monitoring the internal chemical transitions of the devices in the field. To date, to our best knowledge, the only non-destructive analysis of solar cell devices was demonstrated using Terahertz scanning reflectometry. The technique provided information about the concentration of different dyes across the depth of the film using 0-1167 cm^{-1} (0-35 THz) spectral range. [17] Micro-Spatially Offset Raman Spectroscopy (micro-SORS) is an additional analytical approach with different molecular response yielding generally higher chemical specificity, e.g. enabling also to characterise much broader wavenumber regions including fully the important molecular fingerprint region which could be useful in some applications in the concerned application context. For our study, the non-destructive measurements were carried out using micro-SORS, [18-19] a technique that combines SORS [20] and microscopy, permitting the molecular identification of compounds present under the surface (at the micro-

scale), directly from the surface. Such information is otherwise inaccessible to conventional confocal Raman microscopy due to the high optical turbidity of the concerned TiO_2 layer.

Based on its high chemical specificity, in general, micro-SORS was predominantly used to retrieve the composition of superimposed micro-layers. Recently, its use has been extended to the characterization of diffusion of an agent into a turbid matrix ,[21] demonstrating the correlation of the slope of the agent/matrix Raman intensity trend with penetration depth of the agent and its diffusion profile. [22] The investigated diffusion process involved several tens to hundreds micrometers within the matrix, which had an "semi-infinite" (5-10 millimetres) overall thickness, not to impede photons migration processes in z direction (depth). The study of diffusion process is directly related to assessing depth profile of the dye of the power conversion systems. A novel aspect here is the fact that the diffusion process involves only 3-17 μm thickness, with a matrix being only 8-17 μm thick – more than an order of magnitude smaller scales than used to date. Therefore, apart from extending application space for micro-SORS, we are also exploring new micro-SORS detection limits, with a consequent increase of technique applicability, paving ways in general to impact in fields where thin layers need to be non-destructively investigated, also outside DSSC area. Furthermore, this represents the first demonstration on non-destructive characterisation capability in the solar cell field using micro-SORS.

In this work, completely and partially soaked samples resulting in even and uneven dye concentration profiles with depth, respectively, were analysed using full micro-SORS (Figure 1). In this method, there is a full separation between illumination and Raman collection areas which permits to preferentially collect the Raman photons that are generated under the surface and that re-emerge at the surface with a spatial offset compared to the laser incidence position. [23] The collection of the deeply generated Raman photons allows to retrieve the composition of the material under the surface, and in this specific case it permits to monitor the dye distribution inside the TiO_2 matrix. Full micro-SORS was chosen because it ensures a higher contrast than available from the most basic variant, defocusing micro-SORS, where laser incidence and collection zones are not fully separated. [24]

Micro-SORS proved to be capable of differentiating completely soaked and partially soaked samples even in this challenging situation which is close to the limit of resolution of the technique compared with previous studies carried out with micro-SORS. Moreover, Time-of-Flight Secondary Ion Mass Spectroscopy (TOF-SIMS) measurements were carried out to compare this more widely used, destructive technique with micro-SORS.

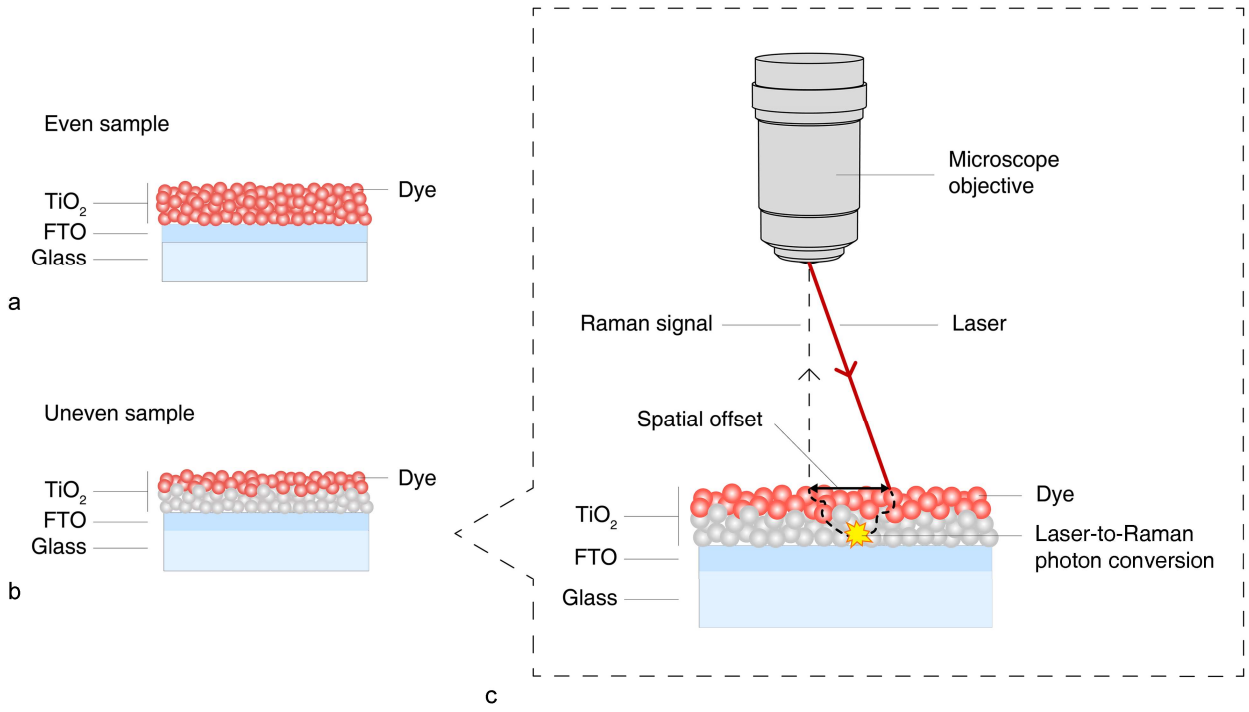

Figure 1. Schematic illustration for samples with even (a) and uneven (b) dye distribution (cross-section view), with the protocol for micro-SORS measurement: the displacement between laser incidence and Raman collection zones allows to collect a Raman photon generated in the inner portion of the TiO_2 film (c).

MATERIALS AND METHODS

Samples preparation

Four photo-electrode samples were prepared, consisting of a TiO_2 film on a fluorine-doped tin oxide glass (FTO, Nippon Sheet Glass Co., Ltd.) and soaked in a solution of dye Y123 (Dyenamo AB). To obtain samples with different characteristics, the thickness of the TiO_2 matrix, the initial dye concentration and the soaking time were varied.

Before the deposition, the FTO glass was ultrasonically cleaned with, in the respective order, acetone, ethanol, and DI water for 10 minutes for each solvent. Mesoporous TiO_2 layers with different thickness were prepared by screen-printing commercial TiO_2 paste (30NR-D, Greatcell Solar Materials Pty. Ltd.) on the cleaned FTO glass, followed by gradual heating at 150 °C for 10 minutes, at 325 °C for 5 minutes, 327 °C for 5 minutes, 450 °C for 15 minutes and at 500 °C for 30 minutes. The average thickness of TiO_2 layer was determined by surface profiler (P6, KLA-Tencor Corporation) as 16.6-µm or 8.2 µm, which are typical TiO_2 thicknesses in DSSCs. (Figure S1 of the Supporting Information). The TiO_2 electrode was immersed in a 50 µM or 100 µM solution of dye Y123 in *tert*-Butyl alcohol/acetonitrile (vol%, 1:1) at room temperature. The

soaking time was varied for obtaining different penetration depths of the dye: longer soaking time (16 h) provided a complete saturation of the film (E, even samples), whereas in the samples with shorter soaking time (1 h) a penetration depth of 3 μm, approximately, was achieved (U, uneven samples). The dye penetration depth was estimated by visual inspection of the samples cross-section using an optical microscope (Leitz Ortholux) after micro-SORS experiments. In Table 1 the list of samples and their features are reported.

Table 1: Label, matrix thickness, soaking time and dye initial soaking concentration of the analysed samples.

Label	TiO_2 thickness (μm)	Dye soaking time (h)	Initial soaking concentration of the dye (μM)
E1	16.6	16	100
U1	16.6	1	100
E2	8.2	16	50
U2	8.2	1	50

Computational details

Geometry optimization and vibrational calculations of the dye Y123 were performed using density functional theory (DFT) calculations with B3LYP functional. The both calculations employed the 6-311G(d,p) basis set without a solvent field. These were implemented with Gaussian 09 D0.1 (Gaussian Inc, Wallingford, CT, USA)[25]. Molecular model for the calculations had shortened alkyl chains to methyl groups for simplifying the calculation process. Dye Raman bands calculation, together with the experimental bands position and their assignment are listed in the Supporting Information, Table S1.

Micro-SORS

Micro-SORS experiments were performed using a Renishaw InVia Raman spectrometer coupled to a Leica DMLM microscope. The measurements were carried out with a 785 nm excitation line, a 50xLWD objective (NA 0.5, a spectral resolution of 1≤ cm^{-1} and a theoretical laser spot diameter of 1.9 μm). Laser power ranging from 0.5 mW to 5 mW and acquisition time of 100s per spectrum were used.

The lateral offset required for the micro-SORS measurements was introduced across the plane of the sample surface using the standard beam-steering optics of the Raman microscope as described earlier. [23] The laser beam was moved by motorized 'beam-steer' alignment mirrors controlled by instrument software. These mirrors are normally used to move the laser spot on sample surface to optimize the overlap of the laser illumination area with the Raman collection area on sample surface for maximizing the Raman signal. Here, the laser spot was moved instead to set the micro-SORS spatial offset. [19]

The measurements were acquired at 0, 3, 5, 7, 10 and 12 μm spatial offsets. The micro-SORS series were collected at different locations on the surface of each sample. The penetration depth of the dye was assessed

by monitoring the relative variation of the intensities of a Raman band of the dye (693 cm^{-1}) and a Raman band of TiO_2 (146 cm^{-1}) with the spatial offset.

The spectral series were first inspected individually to verify the reproducibility of the ratio trends; and then averaged to obtain a representative trend for each sample.

Time-of-Flight Secondary Ion Mass Spectroscopy

The dye distribution throughout the depth in the porous TiO_2 film was obtained using Time-of-Flight Secondary Ion Mass Spectrometry (TOF-SIMS). The TOF-SIMS instrument (TOF-SIMS 5, ION TOF, Germany) was operated with a maximum mass range (> 9,000 amu). The spectra were recorded in the negative ion mode with a mass resolution (m/Δm, >10,000 for Bi^+) under low base pressure (< 5.0×10^{-10} Torr). The dual beam mode was used to carry out the depth profiling. For the dual beam mode, the first ion beam (Cs, 2 keV) was used to mine the broad area (200×200 μm^2). The subsequent second analytical ion beam (Bi_1, 25 keV) was incident to analyse the bottom of the pit in the desired area (50×50 μm^2).

RESULTS AND DISCUSSION

Micro-Spatially Offset Raman Spectroscopy (Micro-SORS)

To study the dye depth profile of dye-sensitized porous TiO_2 films, four types of samples were prepared with different TiO_2 layer thicknesses and dyeing times (Table 1). They can be classified into two groups, even and uneven as described in Figure 1.

The dye distribution in the TiO_2 film was non-destructively studied using micro-SORS. The measurements comprised the acquisition of Raman spectra on the samples surface, starting with a conventional Raman spectrum (zero spatial offset), and then progressively moving the laser away from the Raman collection zone (offset measurements). For the offset measurements, the contribution of the subsurface Raman signal is progressively more pronounced compared to the surface signal, and this permits to retrieve the composition of the more internal portions of the sample.

The Raman spectra collected on the surface of the samples, without any displacement between the laser incidence and the collection zones (zero offset spectra, Figure 2) provide the snapshot of the composition of the most surface region of the sample. All the spectra show the Raman signatures of the red dye (1200, 1188, 1182, 1082, 1000, 930, 920, 793, 693, 583, 466 and 407 cm^{-1}) and anatase, one of the mineral forms of TiO_2 (638, 514, 403 and 146 cm^{-1}). The chemical structure of dye Y123 and detailed Raman band assignments are listed in the Supporting Information (Figure S2, Table S1 and Table S2).

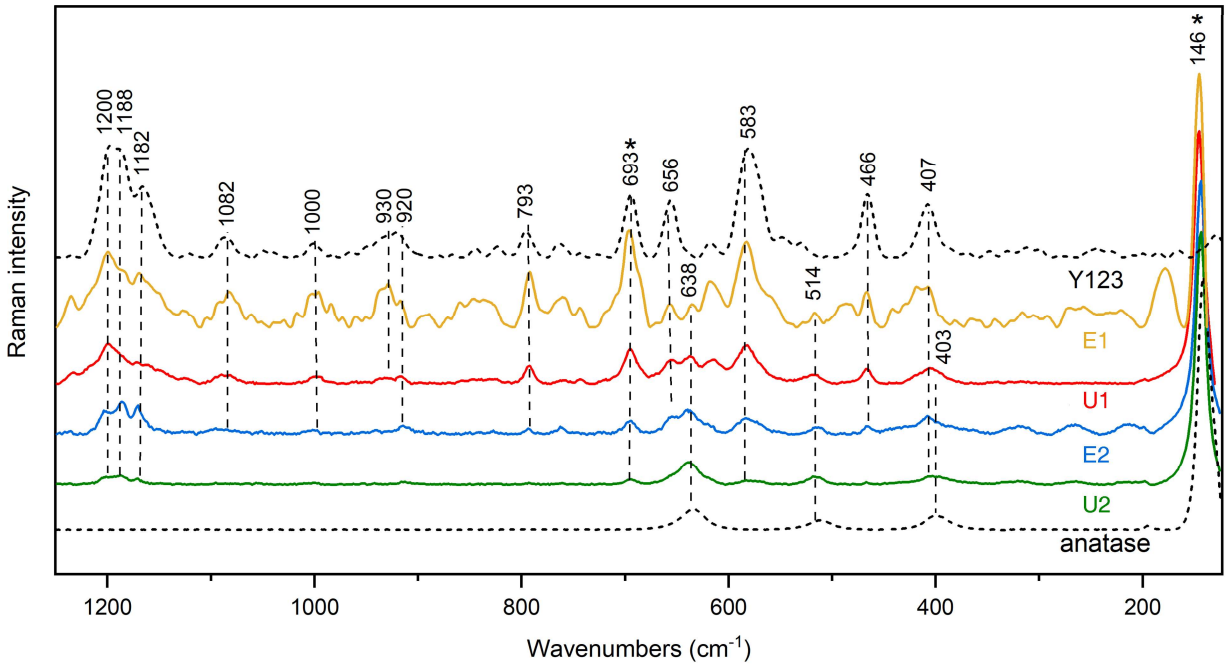

Figure 2. Raman spectra collected at 0 spatial offset on the surface of E1, U1, E2, U2, normalized to the 146 cm^{-1} Raman band of TiO_2 (anatase). The reference spectra of the dye and anatase are reported in black. The asterisks indicate the Raman band used for the intensity ratio calculations.

Interestingly, the 'even' sample E1, prepared with 100 mM dye concentration, shows the most intense Raman bands of the red dye; the 'uneven' sample U1 prepared with the same dye concentration, exhibits comparatively a lower dye intensity at 0 offset. This indicates that, besides the Raman photons generated at the surface, the collection involves a noticeable amount of deeper generated Raman photons (>3 µm) at the '0 offset' resulting in the higher dye signal of E1 compared to U1. Similarly, the even sample E2 shows a more intense Raman signal compared to the uneven sample (U2) prepared with the same initial dye concentration (50 mM). Moreover, E2 and U2Raman spectra show less intense bands of the dye compared to E1 and U1 because a less concentrated dye solution (50 mM) was used for their preparation.

For what concerns the micro-SORS series, the even samples (E1 and E2) show a quite constant dye/anatase Raman intensity ratio with increasing spatial offset. On the contrary, the uneven samples (U1 and U2) display a rapid decrease of the dye Raman bands compared to those of anatase. The Raman spectra of a representative micro-SORS series performed on E1 and U1 are shown (Figure 3). The samples E1 and U1 exhibited a stronger signal of the dye compared to samples E2 and U2, making it easier to visualize the Raman bands intensity change in micro-SORS spectra. The spectra are normalized to the most intense Raman band of anatase (146 cm^{-1}) to better visualize the relative intensity change of the dye Raman bands with the increase of spatial offset as deeper probing takes place: in E1, a slight decrease of the dye Raman bands intensity is observed, possibly related to a small variation of the dye concentration within the TiO_2 matrix.

Conversely, in U1 a dramatic degree of intensity change is observable, resulting from the absence of the dye below the uppermost layer of the film (Figure 3a). Figure 3b focuses on the 660-730 cm^{-1} spectral range, where this behaviour is clearly visible following the intensity change of the dye band at 693 cm^{-1}, that were selected with the 146 cm^{-1} band of anatase for the ratio calculations.

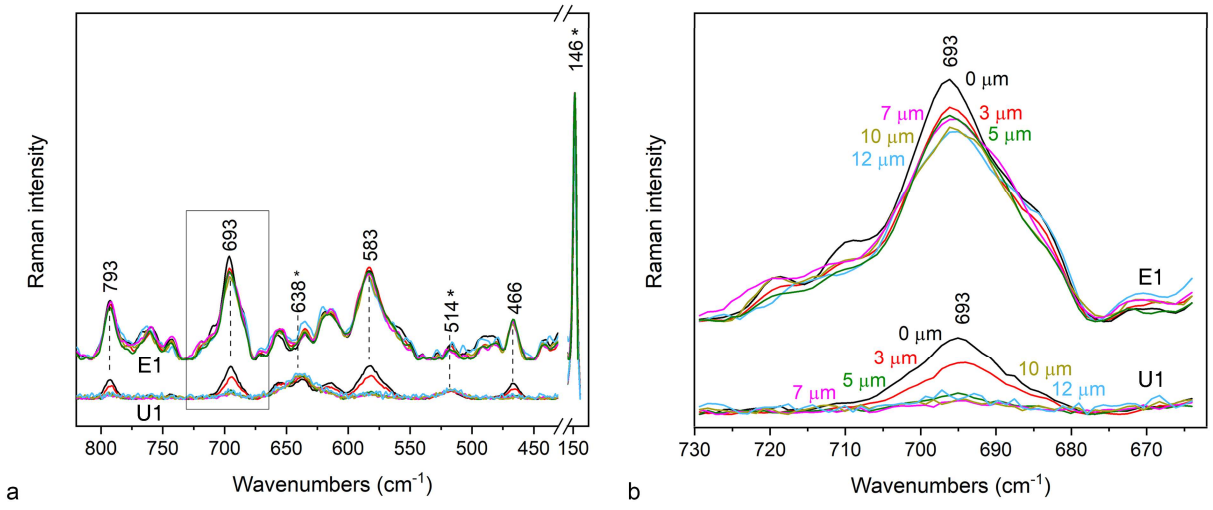

Figure 3. Raman spectra of a micro-SORS series performed on E1 and U1 normalized to the 146 cm^{-1} Raman band of anatase. 110-820 cm^{-1} spectral range, asterisks indicate anatase Raman bands (a). The box frames the spectral range shown in (b) that focuses on the 693 cm^{-1} Raman band of the dye. The spatial offsets are indicated next to the spectra.

The normalized ratio trends of E1 and U1 are shown in Figure 4a, where it is shown that all the series of U1 decrease rapidly with the increase of the spatial offset, whereas in E1 the ratio remains relatively constant. The ratio plot is normalized to the ratio value at 0 offset to make the samples easily comparable. The not normalized ratio plot is shown in Figure S3 of the Supporting Information. All E2 trends are similar to those of the other even sample (E1), and U2 trends show the same rapid decrease observed in U1, as can be visualized in the Figure S4 of the Supporting Information. In Figure 4b, the averaged and normalized ratio trends of all the samples are shown. The ratios of both the even samples (E1 and E2) remain relatively constant with increasing spatial offset, and the uneven samples (U1, U2) exhibit a fast decrease of the ratio value with increasing spatial offset. Therefore, the dye distribution in the TiO_2 layer depends on the dye soaking time greater than the dye solution concentration.

The slope of the linear fit of the ratio curves can be used to easily differentiate the dye distribution behaviours of the samples (Figure 4c). The samples can be separated in two groups based on their slope values: group 1 includes even samples, group 2 uneven samples, demonstrating the micro-SORS capability of distinguishing samples with a partial diffusion of the dye from those completely imbibed, even in the case of a few µm of

penetration depth within thin thickness of the matrix. Moreover, despite the difference in terms of dye Raman bands intensity, resulting from different dye concentration and different manufacturing procedures, the micro-SORS measurements ratio trends behave consistently with the penetration depth of the dye as expected.

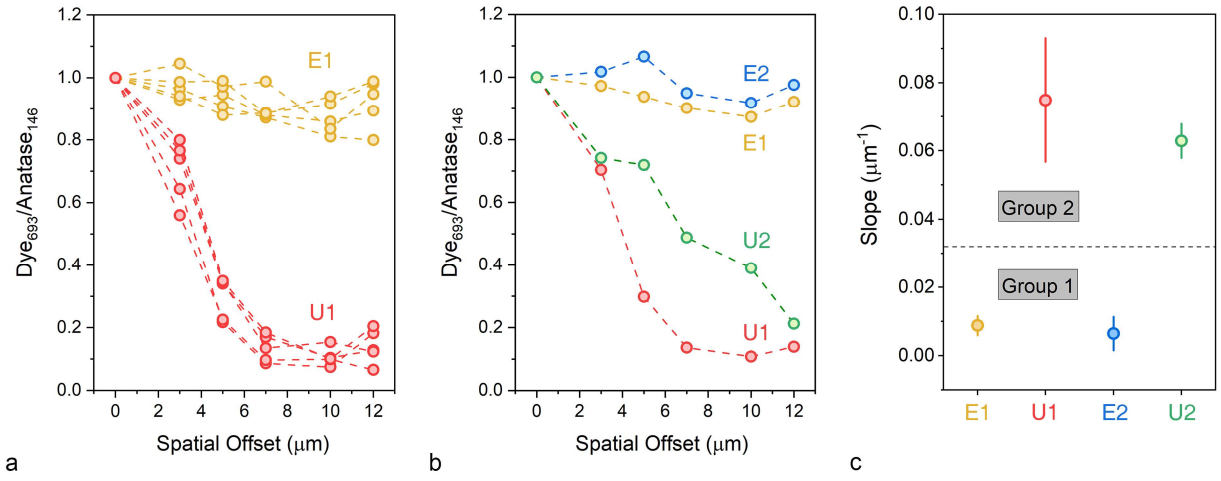

Figure 4: Normalized ratio plots of E1 and U1 (a); normalized ratio plots of E1, U1, E2 and U2 (b); slopes (absolute values) of the linear fitting of the samples ratio trends, with associated confidence intervals (c).

Time-of-Flight Secondary Ion Mass Spectrometry (TOF-SIMS)

To evaluate the reliability of the depth profiling of photo-electrode using micro-SORS, time-of-flight secondary ion mass spectrometry (TOF-SIMS), one of the representative invasive methods, was performed on the TiO_2 films prepared under the same conditions as above. TOF-SIMS extracts mass-to-charge signals of anions at different depths from the surface to the sublayer depending on the time of beam exposure. [16] For both evenly and unevenly sensitized TiO_2 films, the strong TiO^- signal from TiO_2 layer appeared constant before Sn^- and Si^- signals from FTO glass appeared (Figure 5). For the TiO_2 film sensitized for 16 hours (Figure 5a), the CN^- signal from Y123 dye was constantly observed according to the depth, which is consistent with the result of micro-SORS. Moreover, CN^- signal from Y123 dye for the TiO_2 film sensitized for 1 hour (Figure 5b) decreased rapidly with the depth, which demonstrates that the dye was locally sensitized near the surface of the TiO_2 film. These results are in good agreement with the findings of the micro-SORS investigations, supporting the non-invasive applicability of micro-SORS to study dye-sensitized photo-electrodes.

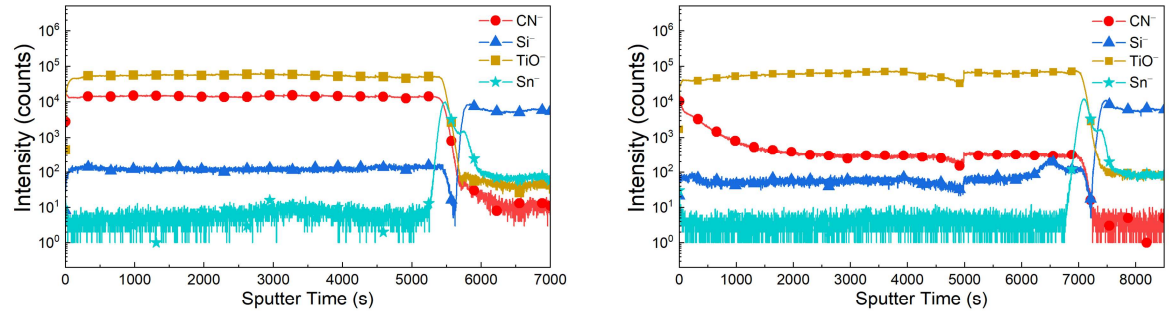

Figure 5: TOF-SIMS depth profiles of Y123-sensitized TiO_2 films according to dye soaking times: 16 hours (a) and 1 hour soaking of TiO_2 in Y123 solution (b). CN^-, Si^-, Sn^-, and TiO^- correspond to Y123, glass, FTO over glass, and TiO_2, respectively. The rapidly decreasing TiO^- and increasing Sn^- signals indicate that the interface between TiO_2 film and FTO was exposed.

CONCLUSIONS

The dye diffusion in photo-electrode was non-destructively studied using micro-SORS for the first time. The method was shown to be effective in discriminating even and uneven samples based on the dye/TiO_2 Raman intensity ratio decay rate with increasing micro-SORS spatial offset. This is important for quality and control purposes in manufacturer of these devices. Micro-SORS and TOF-SIMS measurements provided consistent results, and these findings encourage further investigations on DSSC devices to explore further micro-SORS potential in this field.

Here, the measurements were performed on photo-electrode, but micro-SORS measurements could be potentially performed in-situ, through the glass of an intact solar cell, rendering the analysis completely non-invasive.

The application of the technique could be extended to the monitoring of the temporal degradation of the dye over the device operation which is crucial for the determination of the lifetime of the device.

Moreover, the viability of analysing relatively thin layers (10-20 μm) expands the portfolio of the micro-SORS method, with potential new applications in fields such as semiconductors technology, forensics and pharmaceutics.

ACKNOWLEDGEMENTS

The authors gratefully acknowledge the financial support provided by the 2020 Fundamental Research Development Project funded by Korea Electric Power Corporation (KEPCO) (R20XO02-3), and the National

Research Foundation of Korea funded by the Ministry of Science, ICT and Future Planning (2020R1C1C1014936).

REFERENCES

1. Freitag, M.; Teuscher, J.; Saygili, Y.; Zhang X.; Giordano, F.; Liska, P.; Hua, J.; Zakeeruddin, S.M.; Moser, J.E.; Grätzel, M.l; Hagfeldt, A. Dye-sensitized solar cells for efficient power generation under ambient lighting. *Nature Photon.* **2017**, 11, 372-378

2. Zhang, D.; Stojanovic, M.; Ren, Y.; Cao, Y.; Eickemeyer, F. T.; Socie, E.; Vlachopoulos, N.,ù; Moser, J.E.; Zakeeruddin, S.M.; Hagfeldt, A.; Grätzel, M. A molecular photosensitizer achieves a V_{oc} of 1.24 V enabling highly efficient and stable dye-sensitized solar cells with copper(II/I)-based electrolyte. *Nat. Commun.* **2021**, 12, 1777

3. Hagfeldt, A.; Boschloo, G.; Sun, L.; Kloo, L.; Pettersson, H. Dye-Sensitized Solar Cells. *Chem. Rev.* **2010**, 110, 11, 6595 –6663

4. Kim, B.-M.; Lee, M.-H.; Dilimon, V.S.; Kim, J.S.; Nam, J.S.; Cho, Y.-G.; Noh, H.K.; Roh, D.-H.; Kwon, T.-H.; Song, H.-K. Indoor-light-energy-harvesting dye-sensitized photo-rechargeable battery. *Energy Environ. Sci*. **2020**, 13, 1473-1480

5. Lee, M.-H.; Kim, B.-M.; Lee, Y.; Han, H.-G.; Cho, M.; Kwon, T.-H.; Song, H.-K. Electrochemically Induced Crystallite Alignment of Lithium Manganese Oxide to Improve Lithium Insertion Kinetics for Dye-Sensitized Photorechargeable Batteries. *ACS Energy Lett.* **2021**, 6, 1198-1204

6. Li, S.; Li, Z.-J.; Yu, H.; Sytu, M. R.; Wang, Y.; Beeri, D.; Zheng, W.; Sherman, B. D.; Yoo, C. G.; Leem**,** G. Solar-Driven Lignin Oxidation via Hydrogen Atom Transfer with a Dye-Sensitized TiO_2 Photoanode. *ACS Energy Lett.* **2020**, 5, 777-784

7. Brady, M.D.; Sampaio, R.N.; Wang, D.; Meyer T.J.; Meyer, G.J. Dye-Sensitized Hydrobromic Acid Splitting for Hydrogen Solar Fuel Production. *J. Am. Chem. Soc.* **2017**, 139, 15612-15615

8. Sherman, B.D.; Sheridan, M.V.; Wee, K.-R.; Marquard, S.L.; Wang, D.; Alibabaei, L.; Ashford, D. L.; Meyer, T.J. A Dye-Sensitized Photoelectrochemical Tandem Cell for Light Driven Hydrogen Production from Water. *J. Am. Chem. Soc*. **2016**, 138, 16745-16753

9. Yu, Z.; Lia, F.; Sun, L. Recent advances in dye-sensitized photoelectrochemical cells for solar hydrogen production based on molecular components. *Energy Environ. Sci*. **2015**, 8, 760-775

10. Lee, K.; Park, S. W.; Ko, M. J.; Kim, K.; Park, N.-G. Selective positioning of organic dyes in a mesoporous inorganic oxide film. *Nat. Mater.* **2009**, 8, 665-671

11. Abrusci, A.; Ding, I-K.; Al-Hashimi, M.; Segal-Peretz, T.; McGehee, M.D.; Heeney, M.; Frey G. L.; Snaith, H.J. Facile infiltration of semiconducting polymer into mesoporous electrodes for hybrid solar cells. *Energy Environ. Sci.* **2011**, 4, 3051-3058

12. Ellis-Gibbings, L.; Johansson, V.; Walsh, R.B.; Kloo, L.; Quinton J.S.; Andersson, G.G. Formation of N719 Dye Multilayers on Dye Sensitized Solar Cell Photoelectrode Surfaces Investigated by Direct Determination of Element Concentration Depth Profiles. *Langmuir* **2012**, 28, 9431-9439

13. Yeh, S.-C.; Lee, P.-H.; Liao, H.-Y.; Chen, Y.-Y.; Chen, C.-T.; Jeng R.-J.; Shuye, J.-J. Facile Solution Dropping Method: A Green Process for Dyeing TiO_2 Electrodes of Dye-Sensitized Solar Cells with Enhanced Power Conversion Efficiency. *ACS Sustainable Chem*. *Eng.* **2015**, 3,71-81

14. Gusak, V.; Heiniger, L.-P.; Graetzel, M.; Langhammer, C.; Kasemo, B. Time-Resolved Indirect Nanoplasmonic Sensing Spectroscopy of Dye Molecule Interactions with Dense and Mesoporous TiO_2 Films. *Nano Lett*. **2012**, 12, 2397-2403

15. Gusak, V.; Nkurunziza, E.; Langhammer, C.; Kasemo, B. Real-Time Adsorption and Desorption Kinetics of Dye Z907 on a Flat Mimic of Dye-Sensitized Solar Cell TiO_2 Photoelectrodes. *J. Phys. Chem. C*. **2014**, 118, 17116-17122

16. Kim, B.-M.; Han, H.-G.; Kim, J.S.; Shin, H.O.; Kwon, T.-H. Control and Monitoring of Dye Distribution in Mesoporous TiO_2 Film for Improving Photovoltaic Performance. *ACS Appl. Mater. Interfaces* **2017**, 9, 2572-2580

17. Ghann, W.; Rahman, A.; Rahman, A.; Uddin, J. Interaction of Sensitizing Dyes with Nanostructured TiO_2 Film in Dye-Sensitized Solar Cells Using Terahertz Spectroscopy. *Sci. Rep*. **2016**, 6, 30140

18. Conti, C.; Colombo, C.; Realini, M.; Zerbi, G.; Matousek, P. Subsurface Raman Analysis of Thin Painted Layers. *Appl. Spectrosc*. **2014**, 68, 686-691

19. Mosca, S.; Conti, C.; Stone, N.; Matousek, P. Spatially offset Raman spectroscopy. *Nat. Rev. Methods Prim*. **2021**, 1, 22

20. Matousek, P.; Clark, I. P.; Draper, E. R. C.; Morris, M. D.; Goodship, A. E.; Everall, N.; Towrie, M.; Finney W. F.; Parker, A. W. Subsurface probing in diffusely scattering media using spatially offset Raman spectroscopy. *Appl. Spectrosc*. **2005**, 59, 393-400

21. Botteon, A.; Yiming, J.; Prati, S.; Sciutto, G.; Realini, M.; Colombo, C.; Castiglioni, C.; Matousek, P.; Conti, C. Non-invasive characterisation of molecular diffusion of agent into turbid matrix using micro-SORS. *Talanta* **2020**, 218, 121078

22. Botteon, A.; Realini, M.; Colombo, C.; Conti, C.; Matousek, P.; Castiglioni, C. Micro-SORS, diffusion processes and heritage science: a non-destructive and systematic investigation *Eur. Phys. J. Plus* **2021***,* 136, 880

23. Buckley, K.; Atkins, C. G.; Chen, D.; Schulze, H. G.; Devine, D. V.; Blades, M. W.; Turner, R.F.B. Non-invasive spectroscopy of transfusable red blood cells stored inside sealed plastic blood-bags. *Analyst* **2016**, 141, 1678-1685

24. Conti, C.; Realini, M.; Colombo, C.; Matousek, P. Comparison of key modalities of micro-scale spatially offset Raman spectroscopy. *Analyst* **2015**, 140, 8127-8133

25. Frisch, M. J.; Trucks, G. W.; Schlegel, H. B.; Scuseria, G. E.; Robb, M. A.; Cheeseman, J. R.; Scalmani, G.; Barone, V.; Mennucci, B.; Petersson, G. A. et al. Gaussian 09, revision D.01; Gaussian Inc.: Wallingford, CT, **2013**